

Electrochemical cell studies on fluorinated natural graphite in propylene carbonate electrolyte with difluoromethyl acetate (MFA) additive for low temperature lithium battery application

R CHANDRASEKARAN^{1,*}, M KOH², Y OZHAWA¹, H AOYOMA¹ and T NAKAJIMA¹

¹Department of Applied Chemistry, Aichi Institute of Technology, Yakusa-cho, Toyota-shi 4700392, Japan

²Fundamental Research Department, Chemical Division, Daikin Industries Ltd 1-1 Nishihitotsuya, Settsu-shi, Osaka 5668585, Japan
e-mail: ramachandru70@hotmail.com

MS received 10 June 2008; 4 March 2009

Abstract. Electrochemical cell performances of fluorinated natural graphite (abbreviated as FNG) electrode material was studied by using 1M of LiClO₄·EC:DEC:PC (1:1:1 v/v) electrolyte solution with and without 0.15% v/v fluorinated carboxylic ester additive difluoromethyl acetate–CHF₂COOCH₃ (MFA) at –10°C. The electrochemical cell performances were studied by cyclic voltammetry, galvanostatic charge–discharge and impedance analysis. The additive has proven its positive role with the electrolyte system and has shown the improved characterization over the blank electrolyte system.

Keywords. Lithium battery; low temperature; fluoroester additive; organic electrolyte; natural graphite.

1. Introduction

In recent years, the application of the carbonaceous materials are widely dispersed in all form of the energy storage devices such as lithium battery, fuel cell and capacitor applications due to their safety, low cost, reversible capacity as large as 372 mAh g⁻¹, higher columbic efficiencies and low volume expansion. Natural graphite is one of them and superior than the other forms in terms of its low irreversible capacity at first cycle and it's flat with low potential profile.¹ Usually a mixture of ethylene carbonate (EC): propylene carbonate (PC) or DMC, DEC/dimethyl/diethyl carbonate² is widely adopted electrolyte system, but still lower capacity values at lower temperatures due to their viscosity and solid electrolyte interface (SEI) formation. The PC-based electrolytes are more attractive for low temperature applications, but exfoliation due to its decomposition at graphene layer leads to an irreversible capacity loss (ICL). EC-based electrolyte system has high melting point and a positive approach towards the absence of exfoliation of graphite and good reversible Li-graphite action but failed in low temperature

performances.^{1,3} The SEI formation is responsible for cell reversibility.¹ This SEI effect leads to the decrease of cell efficiency⁴ but the SEI improves the cycling stability, high current rate performances and safety.⁵

The surface composition has obviously a great influence on the graphite anode properties, notably on the value of irreversible capacity since the electrochemical reactions occur at the surface of the electrode. A crucial focus on SEI, several algorithms are introduced for creating SEI precursor for electrodes i.e. the introduction of elements atoms such as fluorine or oxygen on carbon surfaces or modification of carbon surfaces. Some effective methods are, surface fluorination, surface oxidation, metal coating, carbon coating, polymer coating...etc.^{6–12} Surface fluorination is one of the most effective way to modify the surface. Some selective enhancements by surface fluorinations are surface disorder, reaction kinetics, mesopore's expansion of graphite material, which can accommodate more lithium ions, surface area and decomposition potential shift. Fluorinations can normally be attained on the graphite electrode by using CF₄, NF₃, and ClF₃ via the reduction of surface oxygen and increase of the surface disorder for improved electrochemical performances. Surface

*For correspondence

modification by fluorination is mainly dependent on particle size (surface area), it has negative effect in the smaller particle size (high surface area) where as it has a positive electrochemical effect in the case of the higher particle size (low surface area).^{13–16}

The effectiveness of the fluorination was explained at previous research articles. The results show that the effect of fluorination depends on the surface area via the particle sizes of the natural graphite i.e. the higher disorder of the graphite was observed in the case of higher particle size where as the least affect was counted in the smaller particle size. The fluorination effects increase the surface area (or disorder) were obtained in the higher particles size which also shows a better result than the smaller particle size one. The efficiency of the samples was improved by the fluorination where as a small percentile of discharge capacity loss was observed due to the surface disorder.¹⁵

In addition to that, an introduction of additive to electrolyte is a simplest way to minimize the solvent co-intercalation. Recently researchers have successfully proposed some additives. Some of them are HF, CO₂, cyanofuran, *tris*(trifluoroethyl) phosphate (TFP) 1,3-propane sultone, halogenated materials, vinylene carbonate (VC), chloroethylene carbonate (CEC) and vinyl ethylene carbonate (VEC), etc.^{17–27} Fluoroesters, carbonates and acrylates as additives were also examined for lithium batteries so far to improve cell efficiency, electrode stability, electrolyte conductivity, viscosity of electrolyte.^{1,3} Generally, fluorine containing organic electrolyte system is non-flammable. Since many fluorinated co-solvents are analysed to improve the flammability resistance and low temperature applications.²⁸ This proposed candidate purpose mainly concerns for low temperature applications because of the viscosity, ion mobility, high resistivity of electrode and electrode interface are at below expected level.²⁹ For that case, difluoromethyl acetate (MFA) shows a good adaptable electrochemical properties at low temperature especially at cell cycling efficiency. The ester also stands good cycling efficiency in low temperature even if the strong SEI was formed and high temperature profile. Its reduction potential is closely to PC reduction potential. Moreover its decomposition leads to a SEI precursor and it has low viscosity than EC, DEC and PC. MFA also performs a higher thermal stability, stability to lithium metal, single C-F provides better electrochemical performances over multi or branched C-F chains.^{1,28,30,31}

Based on our earlier works,¹ we report the electrochemical cell properties of fluorinated natural graphite at different particle sizes based on 0.15 v% of fluoroester (MFA) in 1 M of LiClO₄-EC:DEC:PC (1:1:1) electrolyte solution to evaluate the performance of MFA activity at -10°C with respect to natural graphite particle size.

2. Experimental

Three kinds of fluorinated natural graphite samples with average particle sizes of 5, 10 and 15 μm (abbreviated to FNG5, FNG10 and FNG15 respectively, (SEC Co., Ltd) were used and their corresponding BET surface areas were 12.1, 7.2 and 5.3 m²g⁻¹ respectively. Surface fluorination was performed by ClF₃ gas (3 × 10⁴ Pa) at 300°C for 2 min in a nickel reactor. ClF₃ was prepared by burning Cl₂ in a fluorine atmosphere at 400°C. The purity of ClF₃ was > 99% after the separation of ClF as a main impurity. The detailed investigation of fluorination was given in our earlier report.¹⁵

Typical working electrode was prepared as follows, the graphite powder was dispersed into 12% wt of poly(vinylidene fluoride) (PVDF) in 1-methyl-2-pyrrolidone (NMP)³² (Kureha Chemical Industry, Co., Ltd. Japan) at ratio of 9:1 by weight basis. A slurry form of the electrode was prepared with the excess of NMP then the slurry was spread onto a desired 1 × 1 cm nickel foam. The coated nickel foam was initially dried in vacuum oven at 120°C and pressed using a hydraulic pump to 10⁻¹ torr pressure. Finally, the electrodes were kept at 160°C for 24 h.

A three electrode cell set-up was used for all electrochemical cell studies based on metallic lithium on nickel mesh (of thickness 0.1 mm) as counter and reference electrodes and the prepared fluorinated natural graphite (FNG) as working electrode. The cells were fabricated in Argon gas (Ar) atmosphere by using home made glass beaker type with 1 mol/dm³ LiClO₄-EC/DEC/PC (1:1:1 v%) (Kishida Chemicals, water content: -10 ppm) with limited percentile of MFA 0.15 v/v% as electrolyte.

The electrochemical analysis were performed by cyclic voltammetry (CV) study which was carried out using an HD model 1200, at scan rate of 0.1 mV/s from 0 V to 2 V, AC impedance analysis which was done with Potentiostat (Solartron, SI1287) with transfer function analyzer (Solartron, model 1255B) at frequency region from 10 to 1 MHz with

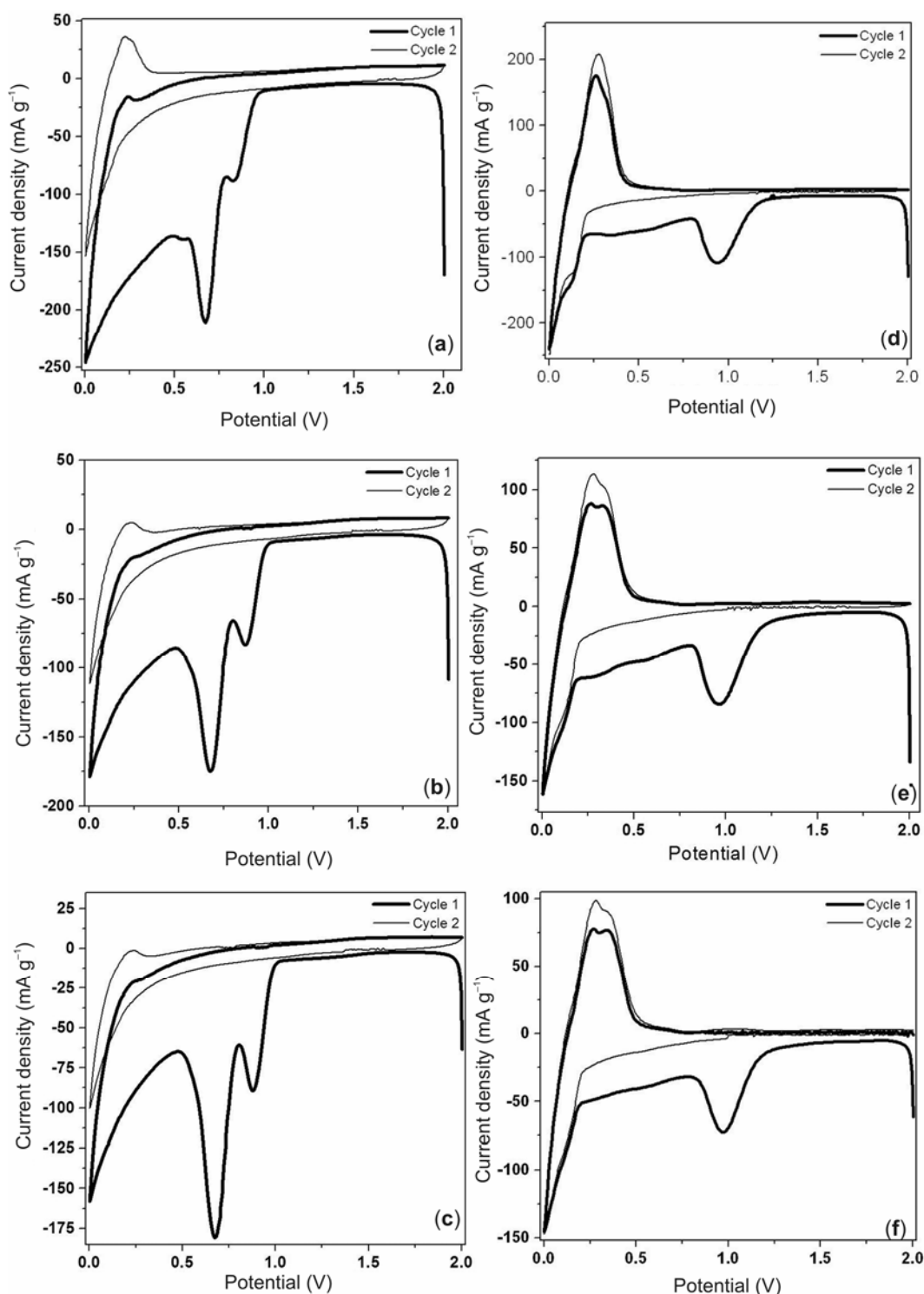


Figure 1. Cyclic voltammograms for FNG5 μm , FNG10 μm and FNG15 μm , obtained at -10°C in $1 \text{ mol.dm}^{-3} \text{ LiClO}_4\text{-EC/DEC/PC}$ (a, b, c) and $\text{-EC/DEC/PC/CHF}_2\text{COOCH}_3$ (d, e, f).

10 mV signal amplitude (before the impedance measurement, the cell was charged nearly to full state of charge at rate of 60 mA/g and kept that level for 30 minute) and Galvanostatic charge–discharge

between 3 and 0 V versus Li/Li^+ at charge rate 60 mA/g with the help of lifecycle tester HJ1001SM8 (Hokuto Denko) with graph plotter. All potentials throughout the manuscript are referred to

metallic lithium reference (Li/Li^+) and the temperature condition was -10°C .

3. Results and discussion

Figure 1 shows the observed cyclic voltammograms for FNGs. Figures 1(d–f) and figures 1(e–f) represent the cyclic voltammograms for the electrodes in 1 M- LiClO_4 -EC/DEC/PC (1 : 1 : 1 v%)-(abbreviated as blank) and 1 M- LiClO_4 -EC/DEC/PC/MFA (1 : 1 : 1 : 0.15 v%)-(abbreviated as MFA system) respectively.

From figures 1a–c, the less anodic and high cathodic features show the heterogeneity of electrochemical Li-ion activity. There was a set of merged reduction peaks for stage 1 (0 to 100 mV) and stage 2 (around 130 mV) Li–C deposition whereas oxidation peaks existence for stage 1 and 2 at 150–270 mV region. The same behaviour was observed in the MFA system. Later, the reversibility of Li was well improved over the blank electrolyte system reversibility, which is clearly evidenced from the oxidation and reduction peak current levels.^{29,33} The reduction current for the stage 1 and 2 involves a considerable fraction of irreversible capacity loss in the case of the blank electrolyte which was confirmed from the broad reduction currents due to increase of electrolyte viscosity at low temperature where as it was minimized in the MFA system.¹ In both cases, there was no decomposition electrolyte peaks in the second cycle shows the stable SEI formation on the electrode surface.⁸

The peak at 0.82–0.88 V in the figures 1a–c was assigned to the decomposition of PC.¹ The reduction peak current due to PC decomposition increases with particle size (as well as sample disorder). Their corresponding reduction potential was shifted to positive potential from the order FNG5 to FNG15. The similar situation was observed for EC decomposition around 0.67 mV which was illustrated in figures 1a–c. No additional decomposition potential position was found in the MFA based system (figures 1(d–f)) in which a peak at 0.94–0.97 mV was assigned for MFA decomposition. The positive potential shifting was also observed in this region from the order FNG5 to FNG15. This EC decomposition on electrode material was almost suppressed by the earlier SEI formation by PC-MFA decomposition product (0.94 mV; figures 1(d–f)) i.e. a short range of decomposition was appeared, which accompanied by the desirable lithium intercalation processes in that SEI barrier.¹⁴

In comparison, the lower current of the first redox couple from the blank electrolyte based cell was due to low diffusion rate of Li^+ ion when compared with MFA system. Generally in the fluoro esters, the decomposition products consist the CF_x groups in SEI facilitates the easy diffusion of Li^+ ion due to low friction of C–F groups.¹ The PC decomposition potentials for FNG10 (0.867 mV) and FNG15 (0.88 mV) were shifted slightly to higher potentials than FNG5 (0.82). The similar changes were noticed in the MFA based cells (0.94 to 0.975 mV). Usually the more surface defect shifts the passivation towards more positive potentials² which was confirmed from the present results. The higher potential decomposition (MFA based cell) shows a driving force for stable SEI formation before the electrolyte decomposition.^{34,35}

A typical impedance plot was depicted in the figure 2 from the charged state of graphite (open circuit potential was kept at zero by galvanostatically). The existence of the small and large semicircle at high-low frequency region (10 kHz to 1 mHz) was evidenced to the SEI formation and charge transfer characterizations respectively. The generalized equivalent circuit representation was given in the figure 2 inset in which R_s , R_{SEI} , C_{SEI} , R_{ct} , C_{ct} and W_c are the electrolyte resistance, resistance from SEI, SEI capacitive component, charge transfer resistance, capacitance at charge transfer region and Warburg factor from the diffusion kinetics. On comparison, there was an observation in the change of resistance

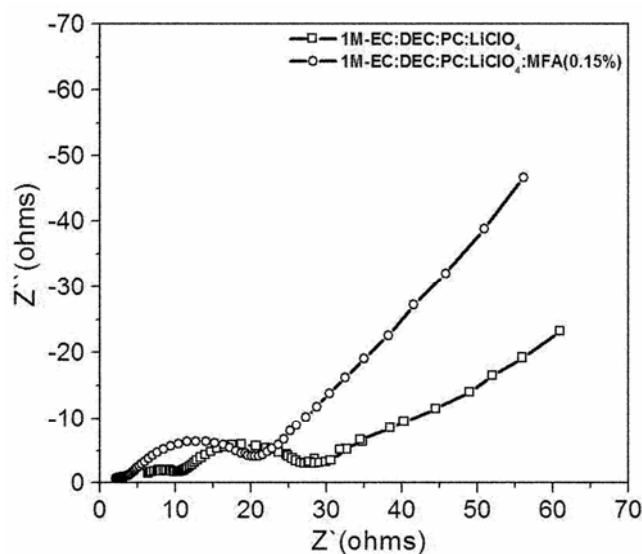


Figure 2. Impedance plot for (a) FNG5 μm at -10°C in 1 mol.dm^{-3} LiClO_4 -EC/DEC/PC and (b) FNG5 μm at -10°C EC/DEC/PC/ $\text{CHF}_2\text{COOCH}_3$.

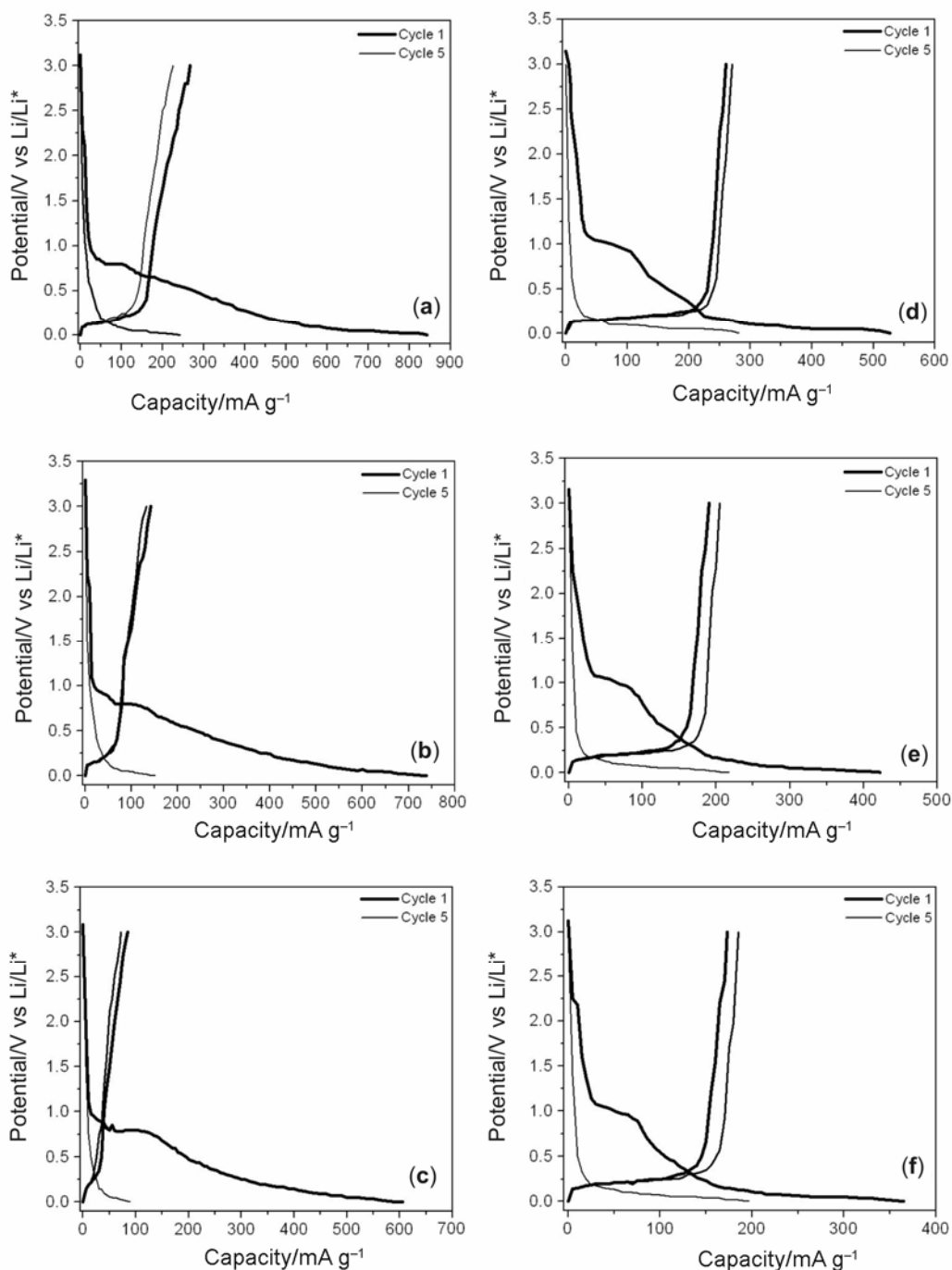


Figure 3. Charge discharge curves for FNG5 μm , FNG10 μm and FNG15 μm , obtained at -10°C in $1 \text{ mol}\cdot\text{dm}^{-3} \text{ LiClO}_4\text{-EC/DEC/PC}$ (a, b, c) and $\text{-EC/DEC/PC/CHF}_2\text{COOCH}_3$ (d, e, f) at constant current density 60 mA/g .

by SEI formation which had lower value for additive based cell i.e. less resistive factor than bare electrolyte system.¹ The MFA additive based cell had a lower solution impedance R_s value (2.76Ω) than the blank system (7.35Ω). The large semi circle represents the charge transfer process of the graphite

material. The charge transfer resistance R_{ct} values also indicate the charge transfer at electrode-electrolyte interface was better in the case of MFA based cell. The R_{ct} approximation values were 17.2Ω (30 mHz region), 16.3Ω for additive free electrolyte and MFA based system respectively.

Both behaviours imply its high rate capability (reducing the electrolyte decomposition) as well as the additive role was cooperative by kinetically.³⁴ Below (30 mHz), the lower frequency region shows the lithium diffusivity behaviour inside the electrode was better than that of the additive free electrolyte system from the slope nature of the curves.³⁶

Figures 3a–f represent the charge–discharge curves, which were observed from the charge and discharge of the fluorinated graphite sample at charge rate of 60 mA/g. The blank electrolyte based cell curves were shown in figures 3a–c where as figures 3 (d–f) shown the MFA based cell curves of cycle 1 and 5. Their corresponding cell efficiencies and cell capacities were presented in figures 4a–b (in text, discharge capacity means graphite alone, if battery means charging process). The measured values were given in table 1.

The calculated capacity loss values of the FNG5, FNG10 and FNG15 electrodes in the blank electrolyte system at SEI region (3.00 V to 0.25 V) were 49.5%, 48.0% and 45.0% respectively, their corresponding capacity loss at intercalation region (0 V to 0.25 V) were 50.5%, 52.0% and 55.0% respectively, where as the capacity losses at the SEI region of MFA based electrolyte were 57.2%, 43.0% and 35.6% and their corresponding capacity loss at intercalation region were 42.8%, 57.0% and 64.3% respectively. The SEI level can attribute this; usually the level increases with surface area increases (indirectly proportional to particle size),^{37,38} but in the case of FNG5 capacity loss was also influenced due to the more MFA reduction co-existence with the solvent decomposition.²⁹ The capacity loss at SEI by FNG10 and FNG15 were well reduced which was the advantage of fluorination over non-fluorinated one, which reflects that the PC decomposition was reduced by increase of surface disorder.¹⁵ The intercalation region was narrowed in the additive based electrolyte when compared to blank electrolyte system, which states that, the decomposition at higher potentials of MFA activate the Li–C interaction or the ionic diffusivity was activated in the SEI regions due to CF_x , MFA decomposition elements.^{1,35} Similar behaviour was observed in the cyclic voltammograms also.

From the table 1, 14–33% of efficiency was improved by MFA addition over the blank system from the order of FNG5 to FNG15 electrode. These efficiency enhancements may be induced by MFA on the activation of the slow rate kinetics,²⁵ which was

also noticed in the figure 1 cyclic curve region from 1.0 V to 0.25 V, means that the decrease of solvent decomposition through stable SEI formation.¹⁵ The possible SEI product for the MFA decomposition may be CHF_2COOLi , which is less soluble in the low temperature but is soluble in high temperature.^{1,28–30} The high level efficiency enhancement has observed in the case of FNG15 and FNG10 system due to their high degree of disorder and surface area where as FNG5 has small efficiency increment.

The low capacity values of FNG10 and FNG15 in the blank electrolyte system were due to their corresponding surface areas (available basal plane and edges were lower). The capacity of FNG10 and FNG15 values was increased drastically in the MFA based system where as it was slightly larger value in the case of the FNG5. The variation strongly depends on particle size and degree of the disorder.

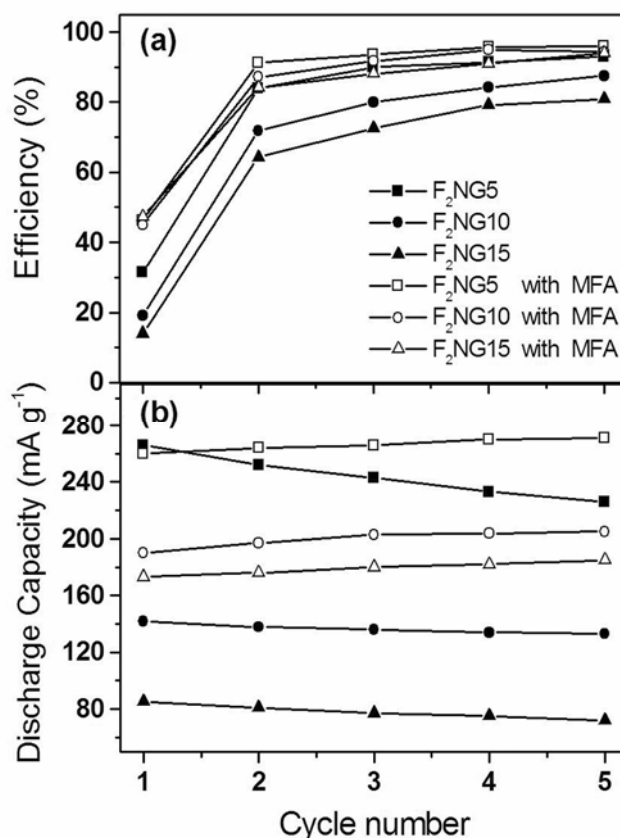


Figure 4. Cell efficiency vs cycle number plot (a) for additive and additive free electrolyte system and their corresponding discharge capacity vs cycle number plot; (b) for additive and additive free system.

Table 1. The discharge capacities and their corresponding cell cycle efficiencies for the blank electrolyte system – EC : DEC : PC and additive based system – EC : DEC : PC : MFA.

Sample	Electrolyte	Discharge capacity (mA/g) with respect to cycle number				
		1 (E%*)	2 (E%)	3 (E%)	4 (E%)	5 (E%)
F ₂ -NG 5	EC : DEC : PC	266 (31.5)	252 (84.0)	243 (90.0)	233 (91.4)	226 (93.0)
F ₂ -NG10	EC : DEC : PC	142 (19.2)	138 (71.9)	136 (80.0)	134 (84.3)	133 (87.5)
F ₂ -NG15	EC : DEC : PC	85 (14.0)	81 (64.3)	77 (72.6)	75 (79.2)	72 (80.9)
F ₂ -NG 5	EC : DEC : PC : MFA	260 (46.3)	264 (91.3)	266 (93.7)	270 (95.7)	271 (96.1)
F ₂ -NG10	EC : DEC : PC : MFA	190 (45.0)	197 (87.2)	203 (91.8)	204 (94.9)	205 (94.5)
F ₂ -NG15	EC : DEC : PC : MFA	173 (47.4)	176 (84.2)	180 (88.2)	182 (91.0)	185 (93.9)

*1(E%) = first cycle cell columbic efficiency

The MFA role was more effective in larger particle size (less surface area graphite samples) than lower particle size (more surface area meets more PC decomposition).³⁹

(i) Overall, the increment of the first columbic efficiencies may be attributed to the earlier decomposition of MFA leads to the minimization of the PC decomposition. (ii) Degree of surface disorder would be an important factor influencing SEI formation. (iii) The flexibility of SEI products in the electrode surface was confirmed from the cycles, after the first cycle the columbic efficiencies attained 80% capacity. (iv) The performances show the MFA based system seemed to provide a sufficient level of merits in efficiency and capacity over the blank electrolyte system. (v) The limitation was implied in the fluorinated system has the gain of capacity depends on the particle size, it has higher value in the case of higher particle size in which it has some percentile efficiency loss due to the disorder of graphite electrode in comparison with non-fluorinated samples.¹

4. Conclusion

The fluorinated electrodes with MFA additive have nominal discharge capacities during the cycling whereas the additive free-based cells have a linear reduction in capacity value, which states that the SEI due to MFA is stable over cycling.

The decomposition of MFA with PC facilitates the lithium intercalation/deintercalation process to and from the graphite electrodes even if it has with SEI formation effect which reflects in cell parameters.

The activity of the MFA for the low temperature applications is selective and preferable for improv-

ing electrochemical activities even though it has failed to obtain practical cell efficiencies at initial cycles.

Acknowledgements

This study was partly supported by a grant from the Frontier Research Project ‘Materials for the 21st century – Materials Development for Environment, Energy and Information’ (for 2002–2006 fiscal years) from the Ministry of Education, Culture, Sports, Science and Technology, Japan. This work was also supported by Daikin Industries, Ltd. Osaka, Japan and SEC Co., Ltd, Japan. The authors gratefully acknowledge their support.

References

- Chandrasekaran R, Ohzawa Y, Nakajima T, Koh M and Aoyama H 2006 *J. New materials for electrochemical systems* **9** 181
- Buqa H, Würsig A, Goers D, Hardwick L J, Holzapfel M, Novák P, Krumeich F and Spahr M E 2005 *J. Power Sources* **146** 134
- Nakajima T, Dan K, Koh M, Ino T and Shimizu T 2001 *J. Fluorine Chemistry* **111** 167
- Lee Y, Yoon C, Prakash J and Sun Y 2004 *J. Electrochem. Soc.* **151** A1728
- Spahr M E, Buqa H, Würsig A, Goers D, Hardwick L, Novák P, Krumeich F, Dentzer J and Vix-Guterl C 2006 *J. Power Sources* **153** 300
- Wang G, Zhang B, Yue M, Xu X, Qu M and Yu Z 2005, *Solid State Ionics* **176** 905
- Schranzhofer H, Bugajski J, Santner H J, Korepp C, Möller K C, Besenhard J O, Winter M and Sitte W 2006 *J. Power Sources* **153** 391
- Zuo X, Xu M, Li W, Su D and Liu J 2006 *Electrochem. Solid State Lett.* **9** A196
- Santner H J, Korepp C, Winter M, Besenhard J O and Möller K C 2004 *J. Anal. Bioanal. Chem.* **379** 266

10. Béguin F, Chevallier F, Vix-Guterl C, Saadallah S, Bertagna V, Rouzaud J N and Frackowiak E 2005 *Carbon* **43** 2160
11. Li J, Naga K, Ohzawa Y, Nakajima T and Iwata H 2005 *J. Fluorine Chemistry* **126** 1028
12. Fu L J, Liu H, Li C, Wu Y P, Rahm E, Holze R and Wu H Q 2006 *Solid State Sci.* **8** 113
13. Groult H, Nakajima T, Perrigaud L, Ohzawa Y, Yashiro H, Komaba S and Kumagai N 2005 *J. Fluorine Chemistry* **126** 1111
14. Fukutsuka T, Hasegawa S, Matsuo Y, Sugie Y, Abe T and Ogumi Z 2005 *J. Power Sources* **146** 151
15. Matsumoto K, Li J, Ohzawa Y, Nakajima T, Mazej Z and Zemva B 2006 *J. Fluorine Chemistry* **127** 1383
16. Tressaud A, Durand E and Labrugere C 2004 *J. Fluorine Chemistry* **125** 1639
17. Korepp C, Santner H J, Fujii T, Ue M, Besenhard J O, Möller K C and Winter M 2006 *J. Power Sources* **158** 578
18. Zhang S S 2006 *J. Power Sources* **162** 1379
19. Naji A, Ghanbaja J, Willmann P and Billaud D 2000 *Electrochim. Acta* **45** 1893
20. Matsuo Y, Fumita K, Fukutsuka T, Sugie Y, Koyama H and Inoue K 2003 *J. Power Sources* **119–121** 373
21. Komaba S, Itabashi T, Kaplan B, Groult H and Kumagai N 2003 *Electrochemistry Communications* **5** 962
22. Lee J, Lin Y and Jan Y J 2004 *J. Power Sources* **132** 244
23. Hu Y, Kong W, Wang Z, Huang X and Chen L 2005 *Solid State Ionics* **176** 53
24. Trofimov B A, Myachina G F, Oparina L A, Korzhova S A, Gusarova N K, Doo S G, Cho M D and Kim H 2005 *J. Power Sources* **147** 260
25. Ufheil J, Martin C, Baertsch C, Würsig A and Novák P 2005 *Electrochim. Acta* **50** 1733
26. Herstedt M, Andersson A M, Rensmo H, Siegbahn H and Edstrom K 2004 *Electrochim. Acta* **49** 4939
27. Wang L, Huang Y and Ji D 2006 *Electrochim. Acta* **51** 4950
28. Ihara M, Hang B, Sato K, Egashira M, Okada M and Yamaki J 2003 *J. Electrochem. Soc.* **150** A1476
29. Nakajima T, Dan K and Koh M 1998 *J. Fluorine Chemistry* **87** 221
30. Yamaki J, Yamazaki I, Egashira M and Okada S 2001 *J. Power Sources* **102** 288
31. Sato K, Yamazaki I, Okada S and Yamaki J 2002 *Solid State Ionics* **148** 463
32. Hossain S, Kim Y, Saleh Y and Loutfy R 2003 *J. Power Sources* **114** 264
33. Noel M and Santhanam R 1998 *J. Power Sources* **72** 53
34. Abe K, Yoshitake H, Kitakura T, Hattori T, Wang H and Yoshio M 2004 *Electrochim. Acta* **49** 4613
35. Wu X, Wang Z, Chen L and Huang X 2004 *J. Surface and Coatings Tech.* **186** 412
36. Funabiki A, Inaba M and Ogumi Z 1997 *J. Power Sources* **68** 227
37. Zaghbi K, Song X, Guerfi A, Kostecki R and Kinoshita K 2003 *J. Power Sources* **124** 505
38. Aurbach D, Levi M D, Levi E A and Schechter A 1997 *J. Phys. Chem.* **101** 2195
39. Chung G C, Kim H J, Yu S, Jun S H, Choi J W and Kim M H 2000 *J. Electrochem. Soc.* **147** 4391